A study of the impact of reduction conditions on molybdenum morphology

J. Bolitschek*, S. Luidold*, M. O'Sullivan**

* Montanuniversität Leoben, 8700 Leoben, Austria

** PLANSEE SE, 6600 Reutte, Austria

Abstract

The current work concerns the influence of different reduction conditions (temperature, dew point and hydrogen content as well as flow rate of reduction gas) on the morphology of molybdenum powder. The material was produced by a two-stage reduction of different sized molybdenum trioxide particles with hydrogen. The experiments were carried out in a rotary kiln. It was found that the specific surface area is mainly influenced by temperature and decreases with rising temperature. The particle size of the raw material, the dew point as well as the hydrogen content of the reduction atmosphere not only have a significant influence on the morphology of the produced molybdenum powder, but also change the impact of the temperature. The results imply that the effect of a single reduction parameter on the properties of the resulting powder always have to be seen in context with the other reaction conditions.

Keywords

Hydrogen reduction, pseudomorphic transformation, chemical vapour transport, molybdenum, molybdenum oxides, morphology, dew point

Introduction

Molybdenum, a refractory metal with a body-centred cubic crystal structure, shows excellent electric, mechanical and thermal properties. Consequently, it finds many engineering applications, for example, in high temperature furnaces, flat panel displays and solar cells. Different processing methods often require feed material with specific features such as porosity, specific surface area (SSA), final content of oxygen and grain size distribution [1–6].

Generally, pure molybdenum is produced via a powder metallurgical approach. Molybdenum trioxide (MoO_3) represents the most commonly used source material for the reduction process for molybdenum metal powder. The production of molybdenum requires two reduction steps, where hydrogen serves as reduction agent. First, MoO_3 is converted to MoO_2 at temperatures around 600–770 °C. This transformation follows the reaction path $MoO_3 \rightarrow Mo_4O_{11} \rightarrow MoO_2$ in an exothermic way. The second

stage occurs at temperatures around 900–1400 °C and involves the endothermic reduction of MoO_2 to Mo [7–11].

Schulmeyer's and Ortner's studies show that the first reduction stage follows a chemical vapour transport (CVT) mechanism under all conditions, whereas the reduction of molybdenum dioxide can be dominated either by pseudomorphic or chemical vapour transport, depending on the dew point (DP). The pseudomorphic transformation occurs at a lower dew point than the CVT mechanism. Throughout the pseudomorphic transformation, the reaction interface moves from the particle surface towards the core of the grain. The product, although showing more pores and pore channels, has a similar shape to the starting material. With an increasing dew point, an intermediate gaseous transport phase (TP) emerges resulting in the development of a new grain morphology [7, 12, 13].

The morphology of the molybdenum powder is mainly determined by the transformation mechanisms occurring in the second reduction step. Accordingly, desirable powder properties can be adjusted through the appropriate choice of reduction parameters [2]. The reaction mechanisms as well as the kinetics of the hydrogen reduction of molybdenum oxides were investigated in several studies [1, 7, 9, 11, 14]. Also, studies examining the effect of reduction conditions on the properties of reduced molybdenum powder have been published. Nevertheless, these studies almost exclusively focus on the impact of the temperature on the outer structure [2, 15, 16]. However, only little information about the impact of other reduction parameters on the surface morphology are described in literature. The focus of this study is on the influence of various reduction parameters, such as the reduction temperature, the dew point, the hydrogen content and the flow rate of the reduction gas on the morphology of molybdenum produced by hydrogen reduction of MoO_3.

Material and experimental procedure

Material

Pure MoO_3 sandy grade powder, supplied by Molibdenos y Metales SA, was used for the experimental process. The raw material is composed of many small rod- to acicular-shaped MoO_3 primary grains (Fig. 1). The material has a specific surface area of 2.35 m^2/g. Three different grain size fractions (63–120 µm, 120–250 µm and > 250 µm) of the feed material were used.

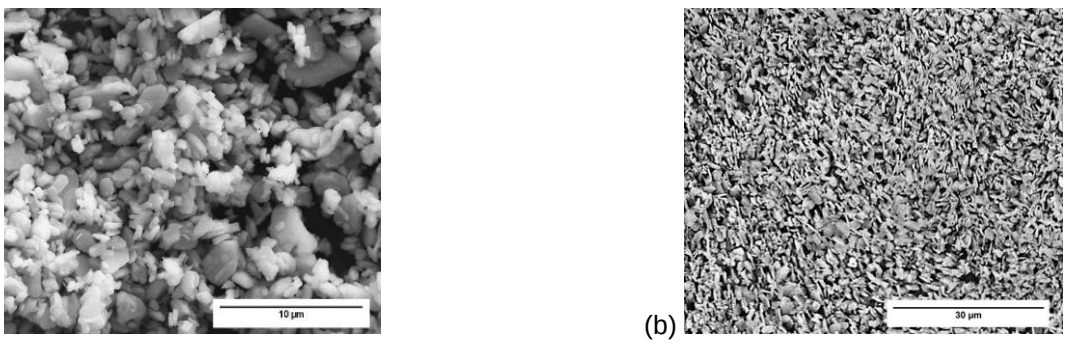

Figure 1: SEM micrograph of the surface morphology (a) and the cross section (b) of MoO_3 used as starting material

Experimental procedures

The reduction experiments took place in a rotary kiln (Nabertherm GmbH) in which a heat-resistant insert, containing the specimens, was rotated at a speed of 3 min^{-1}. The hydrogen gas was humidified by passing it through a temperature controlled bubbler system. Several gas flow meters controlled the flow rates and therefore the gas composition. Fig. 2 shows a schematic diagram of the experimental setup. For each experimental run, 110 g of MoO_3 served as starting material. To achieve fully reduced molybdenum a reduction duration of two hours was required for each reduction stage. The determination of the required reduction duration took place in preparation to this study. A heating rate of 350 °C/h and a reduction temperature of 600 °C for the first stage of reduction was used for all experiments. The parameters dew point of hydrogen (DP), argon content in the atmosphere (Ar) and volumetric flow rate of reduction gases (VFR) were at identical settings for both reduction steps. After the transformation to MoO_2, the specimens were heated from 600 °C to the desired temperatures (850 °C, 950 °C and 1050 °C) for the second reduction step. Consequently, both reduction steps took place in one experimental run, although not in one stage. The reaction started after reaching 550 °C by switching from dry argon to reduction gas and stopped by changing the atmosphere back to argon. The samples cooled to room temperature under an argon atmosphere to prevent a reoxidation of reduced molybdenum. After reaching room temperature, the inlet was taken out of the furnace and the powder removed. For deagglomeration the specimens were grounded in a mortar and particles larger than 250 µm were extracted by sieving.

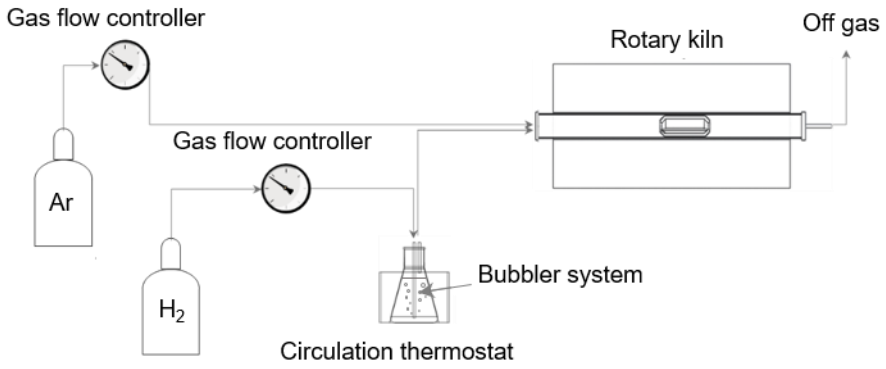

Figure 2: Schematic diagram of the experimental apparatus for the reduction process

Experimental Design and evaluation of results

The object of the present study was to identify the influence of the reduction temperature (T), the particle size of starting material (d50fm), the dew point of hydrogen (DP), the argon content in the atmosphere (Ar) and the volumetric flow rate of the process gases (VFR) on the morphology. The effect of the variables were investigated with a Central Composite Face design of a designed experiment (DoE). In order to gain information on the reproducibility of the experiment, three replicated centre points were included. This design with a total of 26 experiments enabled a quadratic model equation [17]. The experimental setup is given in Table I. The reduction took place under dry (DP = -50 °C) and humidified (DP = 25 °C as well as DP = 50 °C) atmosphere. A higher dew point could not be adjusted due to condensation of water in the gas supply line. The measured responses comprised the specific surface area.

The experimental results were evaluated with the software MODDE 11.0 (MKS Data Analytics Solutions). The fit method multiple linear regression (MLR) was applied and the model was adjusted to obtain maximum values of R^2 (accuracy of fit), Q^2 (accuracy of prediction), model validity and reproducibility [18, 19]. Model terms which showed low significance on the results could be excluded to identify the parameters with the main effect on the responses. However, every single term was included to take significant linear interactions between them into account, even though they had a minor influence on the results.

Characterisation methods

In order to inspect the extent of reduction, hot gas extraction (oxygen/nitrogen/hydrogen elemental analyser ONH 836, LECO) and XRD (D8 Advance, Bruker-AXS) in Bragg-Brentano geometry were conducted. For the XRD analyses, a Cu-Kα radiation and an energy dispersive X-ray detector (Sol-X, Bruker-AXS) were used. The measurement was operated at 40 kV and 40 mA at a range of scattering angle 2θ of $10° < 2\theta < 90°$, a step-width of 0.02° and a measuring time of 1 s per step. The SSA was measured using nitrogen adsorption and the standard multipoint Brunauer-Emmett-Teller method (Nova 2000e, Quantachrome). Additionally, a morphological characterization of the powder by a scanning electron microscope (Quanta 200 Mk2, FEI), employing a secondary electron detector, followed.

Results

The Table I presents the conducted experiments and the results of specific surface area.

X-ray diffraction analysis and hot extraction method

Hot gas extraction and XRD analyses showed that most of the molybdenum oxide powders were completely reduced. In XRD analysis MoO_2 peaks were only detected in specimens produced at 850 °C in an atmosphere containing 60 % argon. However, because only small MoO_2 peaks were observed, all samples could be included in the evaluation of the results.

Influence of reduction conditions on the morphology

Detailed SEM analyses of the molybdenum powder produced revealed the appearance of three different morphologies. The surface morphology and cross section of the specimens are presented in Fig. 3. The sample shown in Fig. 3 (a and d) is an assembly of rod-shaped crystals. On closer inspection each flake is composed of small spherical Mo grains. Additionally, the presence of pores and cracks in the plates was observed. Mainly specimens produced at an atmosphere with a low dew point exhibit this kind of structure. A reduction condition of low dew point was achieved by using a high flow rate of dry hydrogen, a low reduction temperature and a small particle size of the starting material. Consequently, an atmosphere with a high dew point could be created by the use of opposite settings. Predominantly the particles form of fairly loose spherical primary grains, as can be seen in Fig. 3 (b and e), occurred under a condition of a high dew point. The grain size of these spherical grains is larger than the grains produced under dry reduction conditions. Additionally, comparing the coral structure with one another the size of the primary grains decreases with an increasing reduction temperature. Furthermore, a transition morphology developed, which is illustrated in Fig. 3 (c and f) showing a significant amount of pore channels, surface craters and cracks. This shape appeared under various reduction conditions including

Table I: Experimental setup by DoE and achieved results

No.	T [°C]	d50fm [µm]	Ar [%]	DP [°C]	VFR [l/min]	SSA [m²/g]
1	850	101	0	-50	5	1.10
2	1050	101	0	-50	2	0.42
3	850	328	0	-50	2	0.94
4	1050	328	0	-50	5	0.92
5	850	101	60	-50	2	1.06
6	1050	101	60	-50	5	0.87
7	850	328	60	-50	5	0.97
8	1050	328	60	-50	2	0.62
9	850	101	0	50	2	1.42
10	1050	101	0	50	5	0.73
11	850	328	0	50	5	1.93
12	1050	328	0	50	2	0.70
13	850	101	60	50	5	1.67
14	1050	101	60	50	2	0.33
15	850	328	60	50	2	0.61
16	1050	328	60	50	5	0.65
17	850	200	30	25	3.5	1.80
18	1050	200	30	25	3.5	0.75
19	950	101	30	25	3.5	0.86
20	950	328	30	25	3.5	0.94
21	950	200	0	25	3.5	1.23
22	950	200	60	25	3.5	0.75
23	950	200	30	-50	3.5	1.19
24	950	200	30	50	3.5	0.77
25	950	200	30	25	2	0.68
26	950	200	30	25	5	1.17
27	950	200	30	25	3.5	1.77
28	950	200	30	25	3.5	1.64
29	950	200	30	25	3.5	1.42

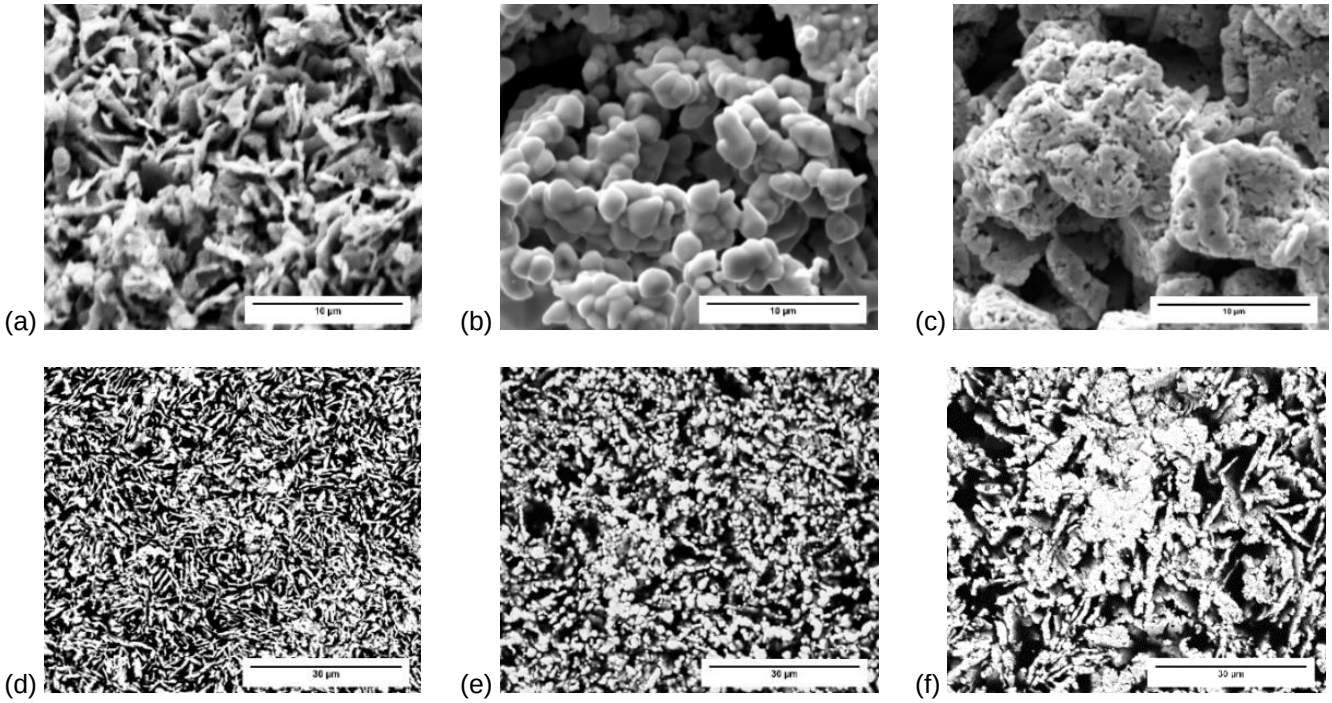

Figure 3: SEM analysis of the change in surface morphology (top) and cross section (bottom) with variation in reduction conditions. (a, d) rod-shaped particles No. 27, (b, e) equiaxed-shaped particles No. 16 (c, f) spongy-shaped No. 3

an average reduction temperature, gas flow rate, argon content in the atmosphere as well as particle size of the starting material.

Studies of the specific surface area

The effect of the reduction conditions on the SSA was studied by using the BET method. The measurements revealed that the SSA of the reduced Mo is smaller than the SSA of the feed material. A complete list of the obtained SSA can be found in Table I. The model possesses a good reliability with a Q^2 value of 0.76 (see Table II), while the equation for predicting the SSA is shown in Eq. 1.

$$SSA = [-1.67 + 4.06 * 10^{-3} * T + 2.68 * 10^{-3} * d50fm + 1.28 * 10^{-3} * Ar - 9.58 * 10^{-3} * DP - 0.18 * VFR + 7.11 * 10^{-6} * d50fm^2 + 0.04 * VFR^2 - 7.15 * 10^{-6} * T * d50fm + 9.80 * 10^{-6} * T * DP - 2.39 * 10^{-4} * T * VFR + 1.38 * 10^{-5} * Ar * d50fm + 1.38 * 10^{-4} * VFR * d50fm + 5.86 * 10^{-5} * Ar * DP + 6.45 * 10^{-4} * Ar * VFR - 3.52 * 10^{-4} * DP * VFR]^2 \quad (1)$$

The prediction plots (Fig. 4 (a)) illustrate the change of SSA with the variation of reduction condition. Each graph describes the influence of one variable on the SSA including the 95 % confidence intervals, while the other parameters were fixed. The effect of every single factor, quadratic effects and interactions on the SSA is presented in Fig. 4 (b). This diagram shows that the temperature and the gas flow rate exhibit the main effects on the SSA. An increase in temperature and a decrease in VFR lead to a decrease in SSA. Moreover, the particle size of the starting material and the degree of humidification of the hydrogen stream show only small effects on the SSA. The inevitable minor condensation of water in the gas supply line at DP > 25 °C could be the reason for the minor influence of humidified hydrogen gas. In conclusion, a decrease of SSA was found by attaining a local high dew point. As reported previously, a high dew point promotes the formation of dense equiaxed-shaped primary grains arranged in a coral structure (Fig. 3 (b)). Due to the dense particles as well as the roundish and smooth structure,

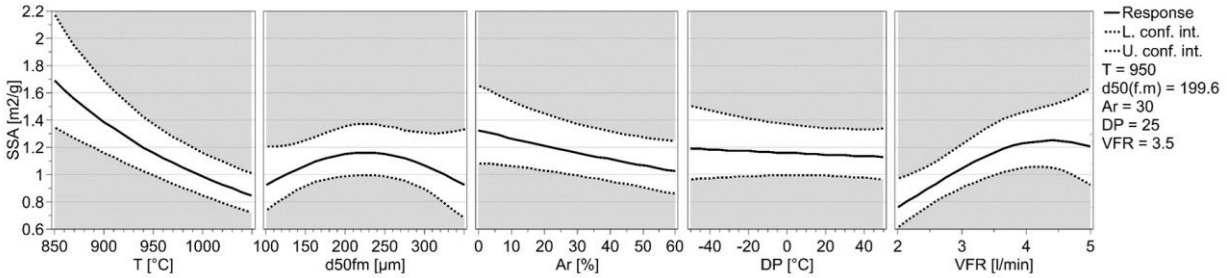

(a)

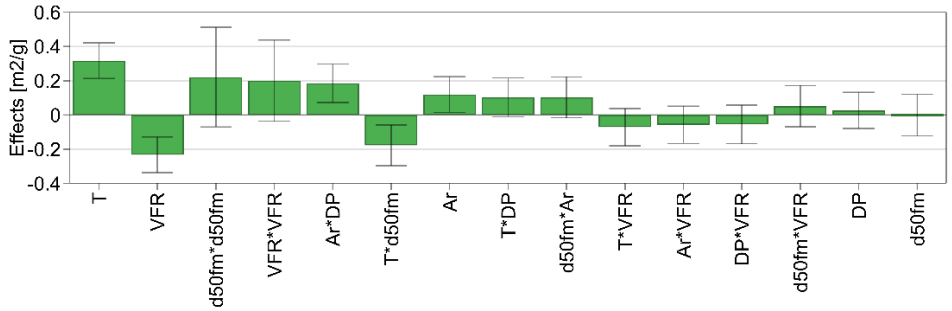

(b)

Figure 4: (a) Prediction plot and (b) effect plot for SSA

Table II: Summary of fit of the model determined by Modde 11

	R^2	Q^2	Model Validity	Reproducibility
SSA [m²/g]	0.91	0.76	0.52	0.96

this kind of particles had the lowest SSA. Specimens showing the transformation morphology (Fig. 3 (c)) just have a slightly higher SSA, due to the pore channels and fissures. Samples consisting of needle-shaped crystals (Fig. 3 (a)) possess a significantly higher amount of porosity and edge cracks and therefore the SSA is almost twice as high.

Considering the statistic evaluation (

Table II), the model validity and accuracy of the prediction can be regarded as good. A high reproducibility, which is the variation of the three centre points in comparison with the overall variability, could be reached for all investigated powder properties. As asserted with the imperfect prediction precision Q^2, a deviation from the future predicted value will arise.

Discussion

This study has shown that the morphology of the molybdenum produced was controlled by different reaction mechanisms, which are influenced by a variation of reduction conditions. The transport mechanisms have been widely researched by Schulmeyer et.al. [7]. According to their studies, second stage reduction conducted at a dew point of hydrogen above 20 °C obeys the chemical vapour transport mechanism, whereas at a low dew point around -40 °C the reaction mechanism corresponds to the pseudomorphic transformation [7]. The development of round particles with a plane surface, which can

be seen in Fig. 3 (b), was benefited through the selection of reduction parameters promoting a high dew point, which supports Schulmeyer's study. The rod-shaped particles, as illustrated in Fig. 3 (a), can be attributed to the pseudomorphic transformation, where the Mo produced retains the shape of the reactant. In comparison to the starting material, more pores and fissures were observed. This finding is in good agreement with Dang's [2] discoveries. The cracks originate from the tensile stress occurring during the decrease in volume, because of the removal of oxygen. Additionally to these two structures, a transitional morphology with a spongy structure was also obtained.

Despite the fact that Majumdar [1] proposed that above the temperature of 900 °C only spherical primary grains occur, we found also rod shaped particles at 950 °C as well as round primary grains at 850 °C. The increased upper limit of temperature for the development of plate-like crystals found in the studies may be due to differences in the other reduction settings. For example, a higher gas flow leads to a faster removal of formed water. As a result, the local dew point is lower and less transport phase can be formed.

As predicted, the coral-shaped morphology possessed the smallest SSA of the three detected morphologies. A reason for this decline is the driving force to minimize the surface energy. Mo atoms from the bulk diffuse to the surface of the particle to annihilate the pores, which leads to a decrease in SSA. Due to the formation of the gaseous transport phase at an increased dew point, a higher mobility of molybdenum atoms is achieved. Therefore, an energetically lower morphology can be achieved more easily. SSA is mainly affected by temperature. This is in complete agreement with Majumdar's discoveries. He reported that the pore annealing and the rounding of the micro particles from a rod to a circular shape is promoted by an increase in temperature [1]. Due to the low temperature and the lack of gaseous transport phase, only few nuclei are formed. Consequently, a structure of large plate-like primary grains was produced. The larger crystals experienced higher stress during the volume decrease through the removal of oxygen, therefore a greater number of pores and fissures appeared. The combination of cracks, pores and fissures as well as a flaky structure are the reasons for the high SSA at low temperature and dew point.

Dang [2] reported that the effect of hydrogen content in the atmosphere on the morphology could be neglected, if one reduction mechanism is dominant. According to him this state should be reached at an extremely low (850 °C) or high (1050 °C) temperature. In our studies different morphologies were created through the change of the hydrogen content as well as other parameters, even at a maximum and a minimum value of temperature.

Conclusion

The results shed light on the influence of the temperature, the particle size of the feed material as well as the dew point, the hydrogen content and the flow rate of the reduction gas on the evolution of morphology during the MoO_3 hydrogen reduction.

The SEM studies showed that depending on the dew point three different morphologies develop. At a very high dew point, the chemical vapour transport mechanism takes place and round dense primary grains are formed. Because of the non-porous and globular primary grains this structure has the lowest specific surface area. At an average dew point both transformation mechanisms take place and a transition system with a sponge-like morphology resulted. Because of the developed pore channels this

showed a slightly higher SSA. Under a dry atmosphere, the particles consist of flake-shaped primary grains, which result from the pseudomorphic mechanism. In this case, the highest SSA was detected. In contrast to earlier findings, the results of the statistic evaluation indicated that not only the temperature but also all the other parameters examined have an effect on the morphological changes of molybdenum. The variation of each factor influences the local dew point and therefore which of the occurring transformation mechanisms predominate.

In order to study the influence of the MoO_2 structure on the produced Mo morphology in detail, future efforts will concentrate on the interaction of the first and second reduction step.

Acknowledgments

The authors gratefully acknowledge financial support by the Austrian Research Promotion Agency.

References

1. S. Majumdar, I.G. Sharma and I. Samajdar, Metallurgical and Materials Transactions B [3], 431–438, (2008)
2. J. Dang, G.H. Zhang and K.C. Chou, High Temperature Materials and Processes [5], (2015)
3. P. Garg, S.J. Park and R.M. German, International Journal of Refractory Metals and Hard Materials [1], 16–24, (2007)
4. M.E. Gaydos, P. Kumar and S. Miller, Methods of making molybdenum titanium sputtering plates and targets, EP2316595 A1, (2011)
5. R.E. Smallwood, Refractory metals and their industrial applications, pp. 3–18, American Society for Testing and Materials, Philadelphia, (1984)
6. ASM International, Properties and selection: Nonferrous alloys and special-purpose materials, pp. 1694–1705, ASM International, Ohio, (2000)
7. W.V. Schulmeyer and H.M. Ortner, International Journal of Refractory metals & hard materials [20], 261–269, (2002)
8. G.P. Martins, T. Kangsadan and G. Scott, Material Science Forum [561–565], 447–452, (2007)
9. B.S. Kim, E.Y. Kim and H.S. Jeon, MATERIALS TRANSACTIONS [9], 2147–2152, (2008)
10. O.D. Neæikov, Handbook of powders of non-ferrous metals, pp. 460–464, Elsevier, Oxford, (2005)
11. J. Dang, G.H. Zhang and K.C. Chou, International Journal of Refractory Metals and Hard Materials, 356–362, (2013)
12. J.Y. Park and O. Levenspiel, Chemical Engineering Science [10], 1207–1214, (1975)
13. R.K. Enneti, International Journal of Refractory Metals and Hard Materials, 122–123, (2012)
14. E. Lalik, W.I. David and P. Barnes, The Journal of Physical Chemistry B [38], 9153–9156, (2001)
15. K. Brookes, Metal Powder Report [2], 18–21, (2004)
16. L. Wang, G.-H. Zhang and J.-S. Wang, The Journal of Physical Chemistry C [7], 4097–4103, (2016)

17. R.H. Myers, D.C. Montgomery and C.M. Anderson-Cook, Response surface methodology, pp. 47–55, Wiley, New Jersey, (2016)
18. L. Eriksson, E. Johansson and N. Kettaneh-Wold, Design of experiments, pp. 76–90, Umetrics AB, Stockholm, (2000)
19. R. Carlson, Journal of Chemometrics [5], 495–496, (2001)